Interface-resolved large eddy simulation of a field debris flow with large stones and woods

Tomoo Fukuda[1*], Shoji Fukuoka[1]

[1] Research and Development Initiative, Chuo University, 1-13-27 Kasuga, Bunkyo-ku, Tokyo 112-8551, Japan.

* Corresponding author. Tel.: +81 3 3817-1617. E-mail address: t-fukuda@tamacc.chuo-u.ac.jp.

1. Introduction

In August 2014, an impermeable check dam was destroyed by a debris flow that occurred in Hiroshima, Japan (see **Fig. 1**). A large amount of huge stones and driftwood attacked a downstream residential area, causing significant damages. In order to countermeasure against the debris flow, it is important to clarify the debris flow and its impact force acting on the check dam. Furthermore, even when the check dam was not filled with stones, there is a possibility that only the driftwood flows out together with the water overflowing the check dam. Therefore, it is necessary to understand not only motions of stones but also that of driftwood. However, it is difficult to measure mechanical property of the debris flow in the field. Consequently, the impact force and the like could not be measured. In the simulation of the debris flow, the mixture of the water and sediment is dealt in general as a continuum. In such models, it is difficult to estimate the segregation of large and small stones, the impact forces of large stones on structures, and the motion of driftwoods different from that of stones.

In our previous study [1], a numerical simulation code for the interface-resolved large eddy simulation (IRLES) was developed. The fluid motion was simulated using the Eulerian approach with smaller computational grids than particles. Motions of particles of various-shapes were simulated as rigid bodies using the Lagrangian approach. For the validation of the model, hyperconcentrated flow in a laboratory experiment was simulated [2]. The particle motions of the simulation result agreed well with those measured in the experiment. Thus, we believe that the implementation of IRLES of field debris flows will reveal dynamics of field debris flows and contribute to understand the debris flow dynamics. However, no effective parallel computation method for the IRLES has been developed so far.

In this study, at first, a wood model is developed by bonding small spheres which is able to drift in the water. Then a new parallel computation technique is developed that is able to reduce computation load by automatically balancing loads of processing elements and is effective for the IRLES of debris flows in complicated boundary geometry. Finally, we introduced the developed wood model and the parallel computational technique to our IRLES code [2], and implemented large-scale IRLES in the upstream 200 m section of the check dam to examine the dynamics of the field debris with large stones and driftwoods (see Fig.1).

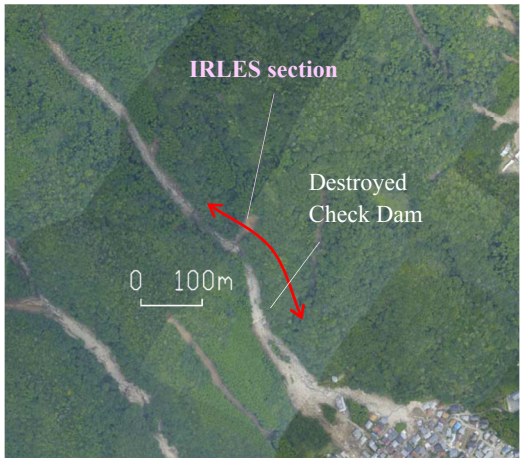

Figure 1. Full view of the objective valley after the debris flow.

2. Numerical methods

2.1. Numerical method of fluid motions

Ushijima et al. [3] developed a single fluid model for the solid-liquid multiphase flows based on the IRDNS (IR direct numerical simulation). In this study, the Smagolinsky model was used as a sub-grid scale turbulence model for the simulation as IRLES (IR large eddy simulation):

$$\frac{\partial u_i}{\partial x_i} = 0 \tag{1}$$

$$\frac{\partial u_i}{\partial t} + u_j \frac{\partial u_i}{\partial x_j} = g_i - \frac{1}{\rho}\frac{\partial P}{\partial x_i} + \frac{\partial}{\partial x_j}\{2(\nu + \nu_t)S_{ij}\} \tag{2}$$

$$\nu_t = (C_s\Delta)^2\sqrt{2S_{ij}S_{ij}} \quad (3)$$

where ρ and u_i are the volume average density and the mass average velocity, respectively, taking into account the volume fraction of the particles in a computation grid. ν is the kinematic viscosity, g_i is the gravitational acceleration, P is the sum of the isotropic components of pressure and SGS stress, S_{ij} is the strain rate tensor, ν_t is the turbulent viscosity, and C_s is the Smagolinsky constant (0.1). Δ is the computation grid size (0.1 m). Simulations of the above equations were performed using the finite difference method of a simplified marker and cell (SMAC) scheme on a staggered grid arrangement. The free water surface was simulated using the volume of fluid (VOF) method [4].

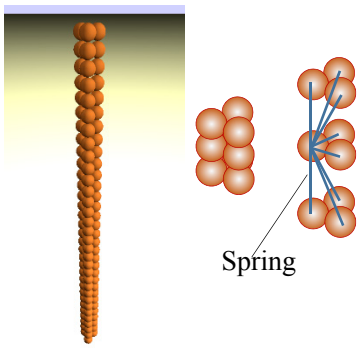

Figure. 2 Wood model

2.2. Numerical method of gravel motions

The gravel-shaped particles were modeled by superimposing several small spheres without gaps. The motion of the particles is simulated using the translational and rotational equations of motion of the rigid body:

$$M\ddot{r}_i = Mg_i + F_i^f + F_i^c \quad (4)$$

$$\dot{\omega}_{i'} = I_{i'j'}^{-1}\left\{R_{j'i}\left(T_i^f + T_i^c\right) - \varepsilon_{j'k'l'}\omega_{k'}I_{l'm'}\omega_{m'}\right\} \quad (5)$$

where, where the index i denots the components of the global coordinate system fixed on the space, the indices i'–m' denote the components of the local coordinate system fixed on a rigid body, M is the mass of a particle, r_i^g is the position of the center of gravity of the rigid body, ω_i is the angular velocity, F_i is the force acting on the surface of the particle, and T_i is the torque on the center of the gravity generated by the force. The superscripts f and c are the components of the fluid forces and contact forces between particles, respectively, g_i is the gravitational acceleration, $I_{i'j'}^{-1}$ is the inverse of the matrix consisting of the components of the moment of inertia tensor in the local coordinate system, $R_{j'i}$ is equal to $\boldsymbol{e}_{j'} \cdot \boldsymbol{e}_i$ ($\boldsymbol{e}_{j'}$ and $\boldsymbol{e}_i$ are unit basis vectors), and $\varepsilon_{j'k'l'}$ is the Levi–Civita symbol.

2.3. Wood model

It is known that the bending deformation of wood makes them easier to accumulate on structures. In this study, to simulate wood deformation, a wood model was developed by using several small spheres that were connected each other using virtual springs (See **Fig. 2**).

2.4. Parallel computation method

A new parallel computation method DBA-BC (dynamic block assignment method taking into account balancing block computation load and shortening communication times) was developed in this study. As shown in the **Fig. 3**, the entire computation domain is divided into cubic domain blocks. Each MPI Processing Element (PE) computes one or more domain blocks. At regular intervals, blocks are virtually assigned to a process in trial a plurality of times by using random numbers. Then, from the virtual trial assignments, only a new assignment of blocks to the PEs is selected that was predicted to shorten the total computation time $T_b + T_c$ (see **Fig. 4**) by balancing computation loads of the blocks T_b among the PEs and shortening communication time T_c that was predicted by using counted the number of communication patterns C_p (see **Fig. 5**). In this manner, this parallel computation technique automatically exchanges blocks among PEs and is able to shorten computation time.

3. IRLES of the field debris flow

3.1. Simulation condition

The domain of the IRLES are shown in **Fig. 6**. The simulation domain was set using 1,978 cubic domain blocks of 5 m each side. The particle size distribution of the simulation was set according to the measured field gravel size

after the debris flow (see **Fig. 7**). Particles of 5 different sizes (0.4, 0.5, 0.6, 0.8, and 1.2 m) were used in the simulation. The smallest particle size of 0.4 m was selected to reduce the computational load. Using these particles, particles were packed in to the valley to reproduce the topography before the debris flow (see **Fig. 8**).

In order to determine the debris volume from the upstream end boundary, a two-dimensional debris flow simulation was carried out. The flow rate of the debris flow Q_m and the volume ratio of solid phase α_s' at the upstream end of the IRLES domain were obtained. However, the volume ratio of solid α_s' obtained from the two-dimensional simulation implicitly includes the fraction of small particles like sand and silt that were not simulated by the IRLES. In the preliminary IRLES in which all of volume ratio as large particles of 30 cm or more, the simulated debris flow tended to accumulate in the vicinity of the upstream end due to great resistance of the large particles. For this reason, the fluid phase in the IRLES was simulated as a mixture of small particles and water of density $\rho_w = 1{,}600\text{kg/m}^3$. The volume ratio of stones of 0.4 m or more α_s, which was simulated in this study using the Lagrangian approach, was determined so that the total volume and mass were consistent with the results of the two-dimensional analysis as follows ($\rho_w' = 1{,}000\ \text{kg/m}^3$, $\rho_s = 2{,}650\ \text{kg/m}^3$):

$$\rho_s\alpha_s + \rho_w(1-\alpha_s) = \rho_s\alpha_s' + \rho_w'(1-\alpha_s')$$

$$\leftrightarrow\ \alpha_s = \alpha_s' + (1-\alpha_s')\frac{\rho_w'-\rho_w}{\rho_s'-\rho_w} \qquad (6)$$

Fig. 9 shows the temporal changes in the flow rate of small sediment laden flow and that of stones supplied from the upstream end of the IRLES.

3.2. Flow configuration

Fig. 10 shows a snapshot of the front of the simulated debris flow. By dealing small particles and water as a mixture continuum, the simulated debris flow was not deposited around the upstream end and violently flew down. Furthermore, woods were plucked out at the frontal portion of the simulated debris flow. This made great wood

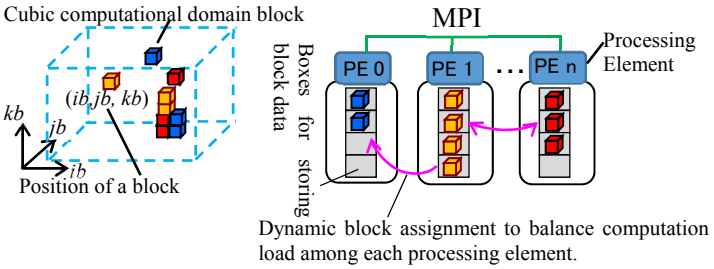

Figure 3. Schematic diagram of DBA.

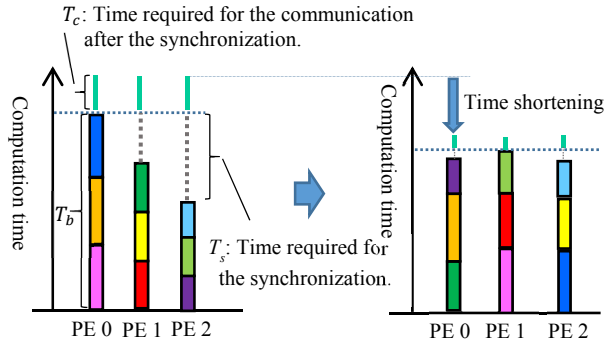

(a) Before the dynamic load balance. (b) After the dynamic load balance.
Rectangles indicate computational times.
Different colors indicate different blocks.

Figure 4. Schematic diagram of computation time before and after dynamic load balance.

C_p A number of communication patterns (Twice the number of arrows)
Equation predicting T_c : $T_c = a_0 + a_1 C_p$
a_0 and a_1 are determined by the least squares method.

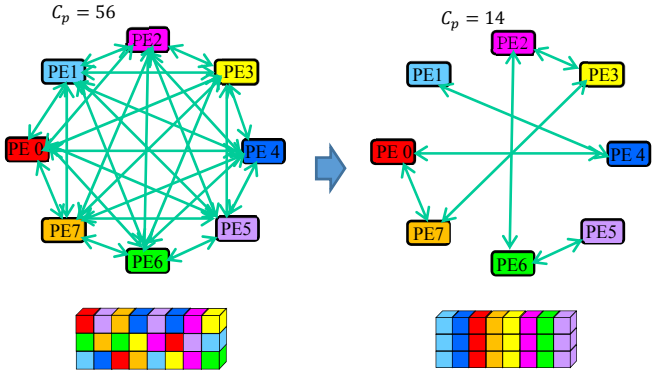

(a) Blocks of the same processing elements are not adjoining.
(b) Blocks of the same processing elsemnts are adjoining.

Figure 5. Communication patterns depending on the assignments of blocks to processes.

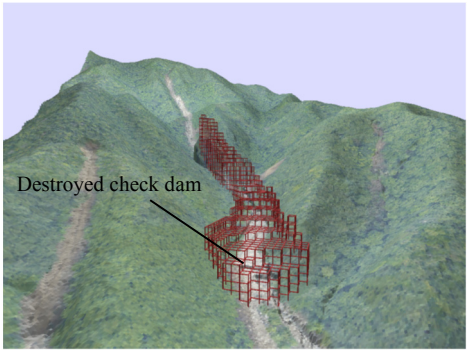

Figure 6. Cubic blocks determining the IRLES domain.

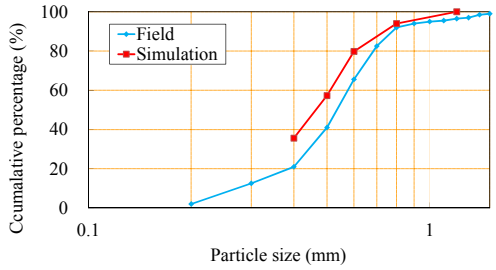

Figure 7. Particle size distribution.

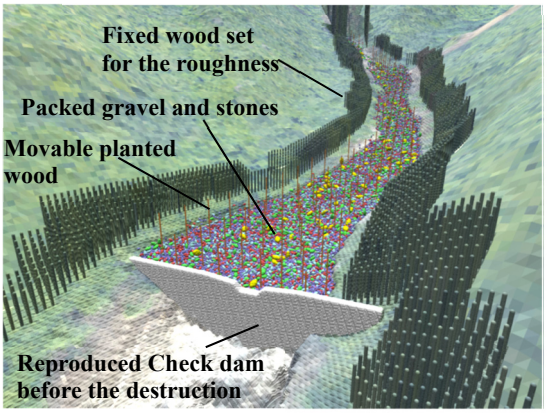

Figure 8. Reproduction of the bed condition before the debris flow.

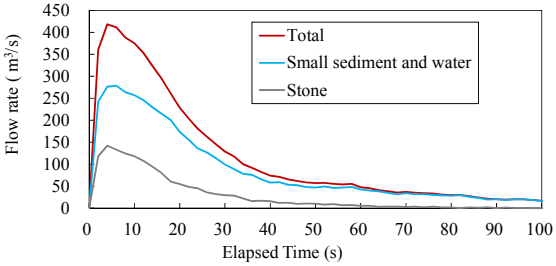

Figure 9. Given flow rates at the upstream end.

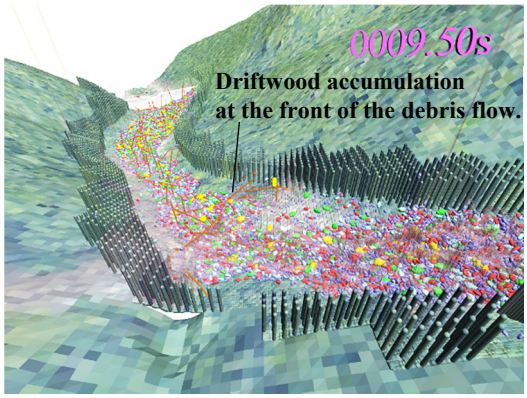

Figure 10. Snap shot of the front of the debris flow.

accumulation at the front of debris flow. Large stones followed the wood accumulation. This phenomenon was recorded by the video shooting on field debris flows. Thus we believe that this IRLES was able to reproduce the flow mechanism of field debris flows.

4. Conclusion

In this study, a deformable wood model was developed. Moreover, a parallel computation method was also developed that was able to dynamically balance the loads of processing elements and suitable for IRLES in complicated boundary geometries. In this way, the IRLES of the field debris flow with large stone and woods was carried out. The simulation were able to predict wood accumulation at the front of the debris flow followed by large stones that was seen in field debris flows. In addition, this phenomenon is difficult to be explained in debris flow continuum model. Thus, the developed debris flow IRLES model is expected to be an effective tool to examine the impact force acting on the check dam and the barrier effect of the check dam against sediment and driftwood.

References

[1] Fukuoka, S., Fukuda, T., Uchida, T., 2014. Effects of sizes and shapes of gravel particles on sediment transports and bed variations in a numerical movable-bed channel, *Adv. in Water Res.*, 72, 84-96, https://doi.org/10.1016/j.advwatres.2014.05.013.

[2] Fukuda, T., Fukuoka, S., 2017. Interface-resolved large eddy simulations of hyperconcentrated flows using spheres and gravel particles, *Adv. in Water Res.*, https://doi.org/10.1016/j.advwatres.2017.10.037.

[3] Ushijima, S., Fukutani, A., Makino, O., 2008. Prediction method for movements with collisions of arbitrary-shaped objects in 3D free-surface flows, *JSCE J* B, 64(2):128-138. http://dx.doi.org/10.2208/jscejb.64.128.

[4] Hirt, C.W., Nichols, B.D., 1981. Volume of fluid (VOF) method for the dynamics of free boundaries, *J. Comput. Phys.*, 39:201-225. http://dx.doi.org/10.1016/0021-9991(81)90145-5.